IL NUOVO CIMENTO **48 C** (2025) 8
DOI 10.1393/ncc/i2025-25008-3

Colloquia: WPCF-Resonance 2023

Searches for the Chiral Magnetic Effect in Xe–Xe and Pb–Pb collisions with ALICE

Andrea Danu(*) for the ALICE Collaboration

Institute of Space Science, Subsidiary of INFLPR - 409 Atomistilor Street, Magurele, Ilfov, 077125, Romania

received 23 July 2024

Summary. — Measurements of charge-dependent three-particle correlations in Pb–Pb and Xe–Xe collisions at $\sqrt{s_{\mathrm{NN}}} = 5.02$ TeV and 5.44 TeV, respectively, are presented. For Pb–Pb collisions, the event shape engineering technique has been employed in the analysis. Results on the centrality dependence of the three-particle correlator $\gamma_{\alpha\beta} \equiv \langle cos(\varphi_\alpha + \varphi_\beta - 2\Psi_2)\rangle$ (α, β denote the charge sign), used to search for the Chiral Magnetic Effect (CME), are reported in the transverse momentum interval $0.2 \leq p_{\mathrm{T}} < 5.0$ GeV/c within the pseudorapidity range $|\eta| < 0.8$. The charge dependence of $\gamma_{\alpha\beta}$ has similar magnitudes in the two collision systems pointing to large background contributions. It is quantitatively reproduced by the Anomalous Viscous Fluid Dynamics model and by a blast wave model calculation that includes non-CME effects in Xe–Xe collisions. Furthermore, these measurements combined with Monte Carlo Glauber and T$_{\mathrm{R}}$ENTo simulations of the magnetic field are used to estimate the fraction of the CME contribution to $\gamma_{\alpha\beta}$ in Xe–Xe and Pb–Pb collisions.

1. – Introduction

Heavy-ion collisions are used to study the quark–gluon plasma predicted to exist by quantum chromodynamics (QCD) at high temperatures and energy densities. In addition, they were proposed to investigate an important property of the strong interaction, parity violation. It has not been observed yet in strong interactions, even though it is allowed by QCD. Local parity violation might occur in microscopic domains due to the interaction of quarks with topological configurations of the gluonic field which changes the quark chirality. This local chiral imbalance coupled with the strong magnetic field produced by the colliding ions ($B \sim 10^{15}$ T) [1] would manifest as a charge separation along the direction of the magnetic field, a phenomenon called the Chiral Magnetic Effect (CME) [2]. Its magnitude is quantified by the $a_{1,\alpha}$ coefficient in a Fourier decomposition

(*) E-mail: `Andrea.Danu@cern.ch`

of the azimuthal distribution of the produced particles with respect to the second order symmetry plane Ψ_2 [3]

$$(1)\quad \frac{\mathrm{d}N}{\mathrm{d}(\varphi_\alpha - \Psi_2)} \sim 1+2v_{1,\alpha}\cos(\varphi_\alpha - \Psi_2)+2a_{1,\alpha}\sin(\varphi_\alpha - \Psi_2)+2v_{2,\alpha}\cos(2(\varphi_\alpha - \Psi_2))+...,$$

where φ_α is the azimuthal angle of a particle with charge α (+, -). The $v_{n,\alpha}$ coefficients characterize the anisotropic flow, *i.e.*, the conversion of initial spatial asymmetries of the collision to momentum anisotropies of produced particles [4]. The $v_{1,\alpha}$ and $v_{2,\alpha}$ coefficients are called directed and elliptic flow, respectively.

The observation of the CME is experimentally difficult and only possible via azimuthal correlations since $\langle a_{1,\alpha}\rangle = 0$ over many events. Only $\langle a_{1,\alpha}^2\rangle$ or $\langle a_{1,+}a_{1,-}\rangle$ can be measured using two- and three-particle correlators [5, 6]

$$(2)\quad \delta_{\alpha,\beta} = \langle cos(\varphi_\alpha - \varphi_\beta)\rangle = \langle v_{1,\alpha}v_{1,\beta}\rangle + \langle a_{1,\alpha}a_{1,\beta}\rangle + B_{\mathrm{in}} + B_{\mathrm{out}},$$

$$(3)\quad \gamma_{\alpha,\beta} = \langle cos(\varphi_\alpha + \varphi_\beta - 2\Psi_2)\rangle = \langle v_{1,\alpha}v_{1,\beta}\rangle - \langle a_{1,\alpha}a_{1,\beta}\rangle + B_{\mathrm{in}} - B_{\mathrm{out}},$$

where B_{in} and B_{out} represent background contributions projected onto Ψ_2 and perpendicular to it, respectively. While $\delta_{\alpha,\beta}$ is dominated by non-flow (*i.e.*, short range correlations unrelated to Ψ_2, such as inter-jet correlations and resonance decays), the $\gamma_{\alpha,\beta}$ suppresses background at the level of v_2. The largest background contribution comes from local charge conservation (LCC) coupled with elliptic flow [7].

2. – Analysis details

The analyses are performed using data recorded by the ALICE detector [8] during the 2017 Xe–Xe and 2018 Pb–Pb runs at $\sqrt{s_{\mathrm{NN}}} = 5.44$ TeV and 5.02 TeV, respectively. Charged-particle tracks are reconstructed using the Inner Tracking System (ITS) and the Time Projection Chamber (TPC). These detectors cover the full azimuth within the pseudorapidity range $|\eta| < 0.9$. The V0 detector covering $-3.7 < \eta < -1.7$ (V0C) and $2.8 < \eta < 5.1$ (V0A) is used for event selection, triggering, and the determination of centrality and Ψ_2. Pileup and beam-induced background events are removed by applying an offline event selection. Approximately 10^6 Xe–Xe (235×10^6 Pb–Pb) events in the 0–70% (0–60%) centrality interval with a primary vertex position within ±10 cm from the nominal interaction point along the beam line are selected. The charge-dependent azimuthal correlations are measured using charged particles reconstructed by the ITS and TPC in the transverse momentum range $0.2 \le p_{\mathrm{T}} < 5.0$ GeV/c within $|\eta| < 0.8$. The v_2 is measured using the event plane method [3] where the orientation of Ψ_2 is estimated from the azimuthal distribution of the energy deposition measured by the V0A detector. More details about the event and track selection criteria employed in the Xe–Xe analysis can be found in ref. [9].

The event shape engineering technique [10] is used to disentangle background contributions from the CME signal in the Pb–Pb analysis. Events with elliptic flow values significantly larger or smaller than the average are selected based on the magnitude of the second-order reduced flow vector q_2 [11], calculated from the azimuthal distribution of the energy deposition measured in the V0C. Ten event-shape classes with the lowest (highest) q_2 value corresponding to the 0–10% (90–100%) range are investigated for each centrality interval as in ref. [12].

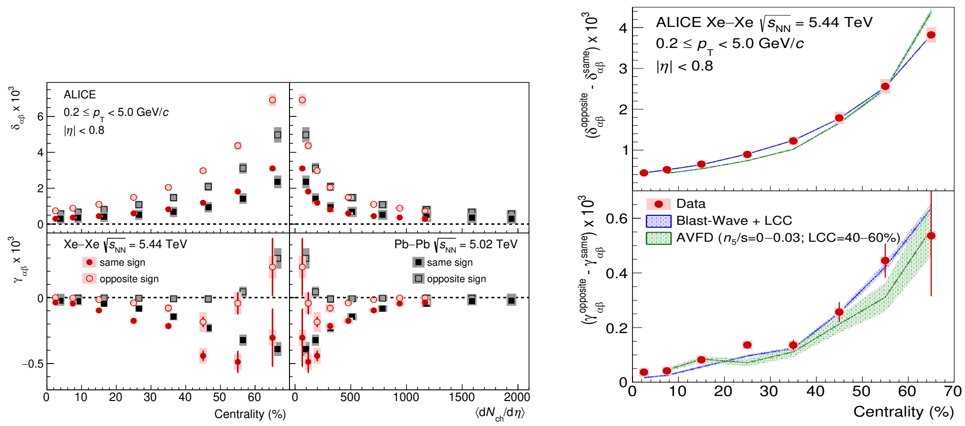

Fig. 1. – Left: Centrality and charged-particle density dependence of $\delta_{\alpha\beta}$ and $\gamma_{\alpha\beta}$ for pairs of particles with same and opposite charges from Xe–Xe and Pb–Pb collisions [9, 13]. Right: Centrality evolution of the charge-dependent difference of $\gamma_{\alpha\beta}$ compared with model calculations: BW parameterization [14] coupled with LCC effects and AVFD [15].

3. – Results

The left panel of fig. 1 presents the $\delta_{\alpha\beta}$ and $\gamma_{\alpha\beta}$ correlators for same- and opposite-charge pairs in Xe–Xe [9] and Pb–Pb [13] collisions at $\sqrt{s_{\rm NN}}$ = 5.44 TeV and 5.02 TeV, respectively, as a function of centrality and average charged-particle multiplicity density $\langle {\rm d}N_{\rm ch}/{\rm d}\eta \rangle$ at midrapidity. Both correlators depend strongly on the charge-sign combination with similar centrality dependence in the two systems. However, the correlations are stronger in Xe–Xe collisions than in Pb–Pb collisions. This might be explained by the different number of particles produced within a given centrality class between the two colliding systems that dilutes the correlations, which is supported by the $\langle {\rm d}N_{\rm ch}/{\rm d}\eta \rangle$ dependence.

The difference between opposite- and same-charge pair correlations for $\delta_{\alpha\beta}$ and $\gamma_{\alpha\beta}$ from Xe–Xe collisions is shown in the right panel of fig. 1. This difference for $\gamma_{\alpha\beta}$ ($\Delta\gamma_{\alpha\beta}$) is used to investigate the charge separation effect. Its magnitude is quantitatively reproduced by a Blast-Wave (BW) parameterization [14] coupled with LCC effects and by the Anomalous Viscous Fluid Dynamics (AVFD) model with values of the CME signal consistent with zero [16]. These observations point to a large background contribution to the measurements in Xe–Xe collisions.

The left panel of fig. 2 shows $\gamma_{\alpha\beta}$ for same- and opposite-charge pairs as a function of centrality for shape selected and unbiased events from Pb–Pb collisions at $\sqrt{s_{\rm NN}}$ = 5.02 TeV. The same-charge correlations are stronger than the opposite-charge correlations for both shape selected and unbiased events. Their magnitudes depend weakly on q_2 (*i.e.*, v_2) within a given centrality class. The v_2 dependence of $\Delta\gamma_{\alpha\beta}$ is presented for various centrality classes in the right panel of fig. 2. The $\Delta\gamma_{\alpha\beta}$ is positive for all centrality intervals and decreases with centrality and v_2 (in a given centrality class). The dependence on v_2 indicates a large non-CME contribution to $\gamma_{\alpha\beta}$.

In order to estimate the fraction of the CME signal to $\gamma_{\alpha\beta}$, denoted as $f_{\rm CME}$, the measured $\Delta\gamma_{\alpha\beta}$ in Xe–Xe and Pb–Pb collisions is combined with Monte Carlo simulations

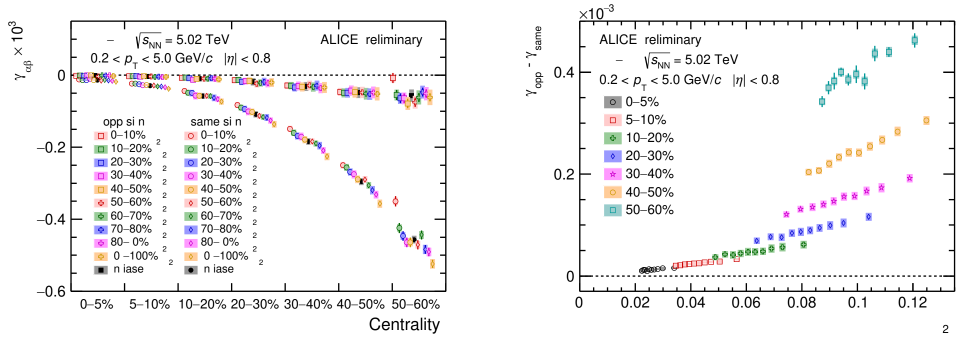

Fig. 2. – Left: Centrality dependence of $\gamma_{\alpha\beta}$ for pairs of particles with same and opposite charges for shape selected and unbiased events from Pb–Pb collisions at $\sqrt{s_{\mathrm{NN}}}$ = 5.02 TeV. Right: $\Delta\gamma_{\alpha\beta}$ as a function of v_2 for shape selected events.

of the magnetic field. The expected centrality and v_2 dependence of the CME signal are estimated from MC Glauber [17] and T$_{\mathrm{R}}$ENTo [18] calculations as detailed in refs. [9,12]. Two different approaches were investigated.

In the first procedure [9], the $\Delta\gamma_{\alpha\beta}$ for the two systems is expressed using a two-component approach by assuming that both the CME signal and background scale with $\mathrm{d}N_{\mathrm{ch}}/\mathrm{d}\eta$

$$\Gamma^{\mathrm{Xe–Xe}} = sB^{\mathrm{Xe–Xe}} + bv_2^{\mathrm{Xe–Xe}}, \tag{4}$$

$$\Gamma^{\mathrm{Pb–Pb}} = sB^{\mathrm{Pb–Pb}} + bv_2^{\mathrm{Pb–Pb}}, \tag{5}$$

where $\Gamma \equiv \gamma_{\alpha\beta}\mathrm{d}N_{\mathrm{ch}}/\mathrm{d}\eta$, $B \equiv \langle (eB)^2 \cos(2(\Psi_{\mathrm{B}} - \Psi_2))\rangle$ ($|B|$ and Ψ_{B} are the magnitude and direction of the magnetic field), and s and b parameters quantify the signal and background contributions, respectively. Extracting s and b from eqs. 4 and 5, one can determine f_{CME} in Xe–Xe and Pb–Pb collisions. The centrality dependence of f_{CME} in Xe–Xe and Pb–Pb collisions is reported in the left panel of fig. 3. The parameter f_{CME} is compatible with zero up to 30% centrality and then becomes positive. Averaging over the centrality range 0–70% gives an upper limit of 2% (25%) at 95% confidence level in Xe–Xe (Pb–Pb) collisions.

In the second approach, the v_2 dependence of $\Delta\gamma_{\alpha\beta}$ and the expected CME signal (*i.e.*, $\langle (eB)^2 \cos(2(\Psi_{\mathrm{B}} - \Psi_2))\rangle$) in Pb–Pb collisions are fitted with a linear function with the slope p_1 being equal to unity in a pure background scenario [12]. Assuming such a case, f_{CME} can be extracted by relating p_1 from data and MC models

$$f_{\mathrm{CME}} * p_{1,\mathrm{MC}} + (1 - f_{\mathrm{CME}}) \times 1 = p_{1,\mathrm{data}}. \tag{6}$$

The right panel of fig. 3 shows f_{CME} for the models employed in this study. The CME fraction cannot be precisely extracted for the 0–5% centrality class. The value of f_{CME} is consistent with zero up to 50% centrality. Combining the points from the 5–60% centrality interval gives an upper limit of 6.4% (5.5%) at 95% confidence level for the MC Glauber (T$_{\mathrm{R}}$ENTo) models.

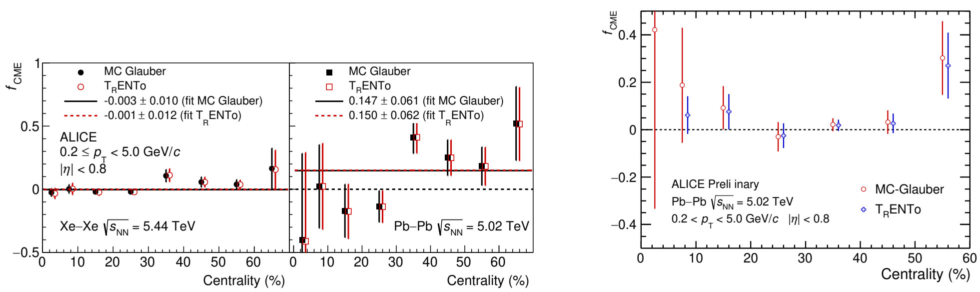

Fig. 3. – Left: Centrality dependence of f_{CME} based on the two-component approach [9] in Xe–Xe and Pb–Pb collisions. Right: Centrality dependence of f_{CME} from the slope parameter of fits to data and MC models [12] in Pb–Pb collisions.

4. – Summary

The charge-dependent three-particle correlator $\gamma_{\alpha\beta}$ has been measured in Xe–Xe and Pb–Pb collisions at $\sqrt{s_{\mathrm{NN}}}$ = 5.44 TeV and 5.02 TeV, respectively. Various observations, including comparisons with MC calculations in Xe–Xe collisions, indicate that the measurements are dominated by background. Different approaches are used to estimate the fraction of the CME signal to $\gamma_{\alpha\beta}$ and the corresponding upper limit in both collision systems.

* * *

This research was partially supported by the Romanian Ministry of Research, Innovation and Digitization under the Romanian National Core Program LAPLAS VII – contract no. 30N/2023.

REFERENCES

[1] Skokov V., Illarionov A. Y. and Toneev V., *Int. J. Mod. Phys. A*, **24** (2009) 5295.
[2] Fukushima K., Kharzeev D. E. and Warringa H. J., *Phys. Rev. D*, **78** (2008) 074033.
[3] Poskanzer A. M. and Voloshin S. A., *Phys. Rev. C*, **58** (1998) 1671.
[4] Ollitrault J.-Y., *Phys. Rev. D*, **46** (1992) 229.
[5] Voloshin S. A., *Phys. Rev. C*, **70** (2004) 057901.
[6] Abelev B. I. *et al.*, *Phys. Rev. Lett.*, **103** (2009) 251601.
[7] Schlichting S. and Pratt S., *Phys. Rev. C*, **83** (2011) 014913.
[8] Aamodt K. *et al.*, *JINST*, **3** (2008) S08002.
[9] Acharya S. *et al.*, arXiv:2210.15383 [nucl-ex] (2022).
[10] Schukraft J., Timmins A. and Voloshin S. A, *Phys. Lett. B*, **719** (2013) 394.
[11] Adler C. *et al.*, *Phys. Rev. C*, **66** (2002) 034904.
[12] Acharya S. *et al.*, *Phys. Lett. B*, **777** (2018) 151.
[13] Acharya S. *et al.*, *JHEP*, **09** (2020) 160.
[14] Retiere F. and Lisa M. A., *Phys. Rev. C*, **70** (2004) 044907.
[15] Shi S., Jiang Y., Lilleskov E. and Liao J., *Ann. Phys.*, **394** (2018) 50.
[16] Christakoglou P., Qiu S. and Staa J., *Eur. Phys. J. C*, **81** (2021) 717.
[17] Miller M. L., Reygers K., Sanders S. J. and Steinberg P., *Annu. Rev. Nucl. Part. Sci.*, **57** (2007) 205.
[18] Moreland J. S., Bernhard J. E. and Bass S. A., *Phys. Rev. C*, **92** (2015) 011901.